Double coupled electron shuttle

M. Prada*
Instituto de Ciencias Materiales de Madrid, ICMM-CSIC, Sor Juana Ines de la Cruz 3, Madrid, Spain
Physics Department, University of Wisconsin-Madison,
1150 University Ave., Madison, Wisconsin 53705, USA and
I. Institut für Theoretische Physik, Universität Hamburg, Jungiusstr. 9, 20355 Hamburg, Germany

G. Platero
Instituto de Ciencias Materiales de Madrid, ICMM-CSIC, Sor Juana Ines de la Cruz 3, Madrid, Spain
(Dated: March 4, 2013)

A nano-shuttle consisting of two movable islands connected in series and integrated between two contacts is studied. We evaluate the electron transport through the system in the presence of a source-drain voltage with and without an rf excitation. We evaluate the response of the system in terms of the net direct current enhanced by the mechanical motion of the oscillators. An introduction to the charge stability diagram is given in terms of electrochemical potentials and mechanical displacements. The low capacitance of the islands allows the observation of Coulomb blockade even at room temperature. Using radio frequency excitations, the nonlinear dynamics of the system is studied. The oscillators can be tuned to unstable regions where mechanically assisted transfer of electrons can further increase the amplitude of motion, resulting of a net energy being pumped into the system. The resulting amplified response can be exploited to design a mechanical motion detector of nanoscale objects.

PACS numbers: 85.85.+j ; 81.07.Oj; 05.45.Xt ; 05.45.–a; 47.20.Ky; 73.23.Hk

I. INTRODUCTION

Recent experiments on coupled shuttles show intriguing effects arising from the coupling of the electrostatics and mechanical degrees of freedom [1, 2]. The imprints of single-electron effects have been observed in these systems, such as Coulomb blockade [3, 4] and gate-voltage-dependent oscillations of the conductance [5]. The increasing relevance of nano electromechanical system (NEMS) is a result of their potential industrial applications [6, 7]. NEMS offer the possibility to realize, for instance, nanomechanical switches [8], circuits [9–11], electronic transducers [12–14], solar cells [15] or high-sensitive charge [1], spin [16] and mass sensors [17, 18], as well as the general study of nonlinear dynamics of oscillators and resonators [19–22]. In particular, there is a growing interest in parametrically driven nonlinear systems [23, 24], where a smooth change in the value of a parameter results in a sudden change of the response of a system.

Our aim is to present here a theoretical study on the electromechanics of a coupled shuttle with an external electrical excitation. The "smoothly" changing parameters are the intensity and the frequency of the excitation, and the response is the observable direct current through the system. In this context, we consider mechanically assisted electron transport through a system of movable low-capacitance nanoislands connected in series between two electrodes. The mechanical motion of the islands changes the mutual capacitance of the system and the tunneling processes, hence affecting the current through the system. We can thus say that the mechanical and electronic degrees of freedom are coupled. An rf excitation allows us to study the effects of nonlinear mechanics, where multiple stability can be achieved by tuning the frequency and intensity of the excitation in the coupled mode regime. In the unstable regions the response of the system is greatly amplified, suggesting a practical scheme for detection of instabilities in the mechanical motion of nanoscale objects.

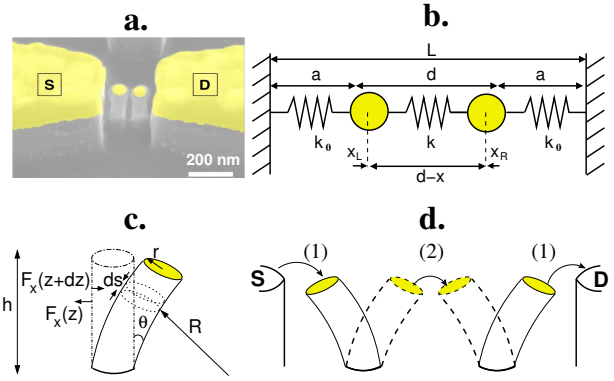

FIG. 1: *(a) SEM image of a coupled shuttle consisting of two Si-based nanopillars, (b) double harmonic oscillator, with coupling spring constants k and k_0, and mechanical displacements x_L and x_R, and (c) forces that generate the displacement x in a differential element* ds *of the nanopillar. (d) The flexural mode where the center of mass is at rest.*

An example of the device that we analyze is the one developed by Kim *et al.* [3], consisting of a double pillar structure with a gold nanoisland on top. [see the SEM image of Fig. 1(a)]. The device can be described in terms of two sets of characteristic quantities. The first one is the relative displacement of the islands, $x = x_L - x_R = r_0 \cos \omega t$ [see Fig. 1(b)], with r_0 being the amplitude of the oscillations and ω the vibration frequency. The mutual capacitances and resistances of the device depend on this quantity, affecting as well the other

*Electronic address: prada@wisc.edu

important set of parameters: the electrostatic free energy for a given charge configuration, $F(m_i)$, where m_i labels the charge state of the device.

This work is organized as follows: in Sec. II, we describe the purely mechanical aspects of the nanopillars in a flexural mode. Sec. III then describes the electrostatics of the system, introducing the free energy and chemical potentials as a function of the mechanical displacements. In Sec. IV we consider the coupling of the mechanical and electronic degrees of freedom. A dynamic equation is derived, and we conclude with a master equation to describe electron transfer processes between the contacts. We evaluate in detail the small oscillations limit and the shuttling regime within the Coulomb blockade limit. We also give an expression for the dissipated and absorbed power by the device. Finally, we devote Sec. V to conclusions.

II. MECHANICAL ASPECTS OF THE COUPLED OSCILLATOR

The system of our interest is represented in Fig. 1. Two nanopillars of height h are operated in a flexural mode where the center of mass remains at rest in most cases, mechanically assisting electronic transport across the system. We consider first a single pillar, as in Fig. 1 (c). The beam can vibrate along x, with displacements $x(z,t)$. A differential element of length dz and cross-sectional area A is subject to forces $F_x(z+dz)$ and $-F_x(z)$ on each face, directed along x, and torques $M_y(z+dz)$ and $-M_y(z)$, directed along y. Balancing linear forces and imposing that there is no net torque [25], we have

$$\begin{aligned} F_x(z+dz)-F_x(z) &= \rho A dz \frac{\partial^2 x}{\partial t^2}, \\ F_x(z+dz)dz + M_y(z+dz) - M_y(z) &= 0, \end{aligned} \qquad (1)$$

where $M_y = EI_x(\partial^2 x/\partial z^2)$, E being the Young modulus and $I_x = \pi r^4/4$, the second moment of area of a cylinder. Expanding about the point z and keeping only first-order terms in dz, we find the Euler-Bernoulli equation (note that we are neglecting the damping force for now):

$$EI_x \frac{\partial^4 x}{\partial z^4} = -\rho A \frac{\partial^2 x}{\partial t^2},$$

with solutions $x_n(z,t) = [a_n(\cos\beta_n z - \cosh\beta_n z) + b_n(\sin\beta_n z - \sinh\beta_n z)]\cos\omega_n t$. With the boundary conditions $x(0,t) = \partial_z x(0,t) = 0$ and $\partial_z^2 x(h,t) = \partial_z^3 x(h,t) = 0$, we find numerically $\beta_n h$ = 1.875, 4.694, 7.855, ..., with $\omega_n = \sqrt{(EI_x/\rho A)}\beta_n^2$ and $a_n/b_n = -1.362, = -0.982, = -1.008, = -1.000, \ldots$ [25]. For the first mode, we can estimate that $\omega_0 \simeq 240$ MHz for a typical nanopillar with a radius $r \sim 30$ nm and using a Young modulus of E = 150 GPa [26]. At the metallic islands situated on top of the pillars ($z = h$), the mechanical movement thus can be described as a harmonic oscillator, $m\ddot{x}_i + \omega_0^2 x_i = 0$.

We now consider the double oscillator in its coupled mode, as depicted in Fig. 1(b). Two harmonic oscillators of mass m and spring constants $k_0 = m\omega_0^2$, with coupling spring constant $k = \varsigma m\omega_0^2$, where ς is a parameter that quantifies the coupling of the oscillators. The dynamics of the system can be derived from its Lagrangian,

$$\mathcal{L} = \frac{1}{2}m\dot{x}_L^2 + \frac{1}{2}m\dot{x}_R^2 - \frac{1}{2}m\omega_0^2\left[x_L^2 + x_R^2 + \varsigma(x_R - x_L)^2\right]. \qquad (2)$$

The problem suggests using the new coordinates, where $X = (x_L + x_R)/2$ is the center of mass and $x = x_L - x_R$, the relative displacement, giving

$$x(t) = r_0\cos(\omega t + \varphi), \quad X(t) = X_0\cos(\omega_0 t + \varphi'),$$

where r_0, X_0, φ and φ' are determined by the initial conditions. We see that the center of mass moves with the natural frequency ω_0, whereas the relative coordinate moves with a higher frequency, $\omega = (1+2\varsigma)\sqrt{k_0/m} = \sqrt{k'/m}$, $k' = k_0(1+2\varsigma)^2$. Two limiting cases can be considered: strong coupling (SC), where $\varsigma \gg 1$, and weak coupling (WC), with $\varsigma \ll 1$. In the SC regime, the movement of one oscillator is quickly transferred to the second, whereas in the WC regime, the movement of the first oscillator is slowly transferred to the second one, which is the situation we expect to encounter in our system.

III. ELECTRODYNAMICS OF TWO METALLIC MOVABLE GRAINS BETWEEN TWO CONTACTS

A. Free energy of movable coupled metallic grains

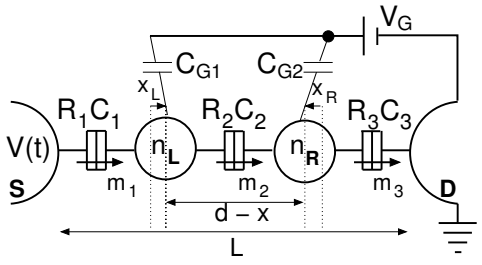

FIG. 2: *A schematic picture of the double-island structure with the voltage sources and various capacities in the system. The two circles denote the islands with $n_{L,R}$ excess electrons. The distance between the islands is given in terms of their relative displacement, $x(t)$. A bias $V(t)$ is applied to the left contact while maintaining the right one grounded.*

The circuit diagram of our system is depicted in Fig. 2: two oscillating, capacitively coupled metallic islands with n_L (n_R) excess electrons in the left (right) island, resulting in a sequence of three tunnel junctions, i = 1, 2, 3, each characterized by a resistance and a capacitance, R_i and C_i. $n_{L,R}$ is determined by the charge accumulation in the junctions, m_i

$$\begin{aligned} n_L &= m_1 - m_2, \\ n_R &= m_2 - m_3. \end{aligned} \qquad (3)$$

A bias $V(t)$ is applied to the left contact, while maintaining the right one grounded.

The capacitances of the (disk shaped) left and right island $C_{L,R}$ and their mutual capacitance C_2 can be expressed in terms of their radii, $r_{L,R}$,

$$C_{L,R} \simeq 8\varepsilon r_{L,R}; \qquad C_2 \simeq 8\varepsilon \frac{r_L r_R}{(d-x)} = C_2^0 \frac{1}{1-x/d}, \quad (4)$$

where d is the equilibrium distance between the islands. Here, ε is the dielectric constant of the material surrounding the electrodes, $\varepsilon = \varepsilon_0 \varepsilon_r$. In our case, $\varepsilon_r \sim 1$ (air), so the dielectric constant is close to the vacuum one, ε_0.

A full derivation of the free energy is given in Appendix A. The free energy in the linear transport regime [*i.e.*, for $V(t) \simeq 0$] in terms of the m_i and n_α given by Eq. (3) reads

$$\begin{aligned} F(\{n_\alpha, m_i\}) &= \frac{1}{2} n_L^2 E_{CL} + \frac{1}{2} n_R^2 E_{CR} + n_L n_R E_{CC} - W(\{m_i\}); \\ W(\{m_i\}) &= \frac{1}{|e|} \{ m_1 [V_G (C_{G1} E_{CL} + C_2^0 E_{CC})] + \\ &+ m_2 [V_G (C_{G1}(E_{CL} - E_{CC}) - C_{G2}(E_{CR} - E_{CC})] \\ &+ m_3 [-V_G (C_{G1} E_{CC} + C_{G2} E_{CR})] \}, \end{aligned} \quad (5)$$

where $E_{CL(CR)}$ is the charging energy of the left (right) island and E_{CC} is the electrostatic coupling energy, which denotes the change in energy of one island when an electron is added to the other island. These energies can be expressed in terms of x, using Eq. (4),

$$E_{CL/CR} = \frac{e^2}{C_{L/R}} \left(\frac{1}{1 - \frac{r_L r_R}{(d-x)^2}} \right); \; E_{CC} = \frac{e^2}{C_2^0} \left(\frac{1}{\frac{(d-x)^2}{r_L r_R} - 1} \right). \quad (6)$$

We note that the charging energy of the individual islands do not change dramatically with the oscillations, since $(d - x) \geq r_L + r_R$ implies (using $r_L \sim r_R = r$) $E^0_{CL/CR} < E_{CL/CR} < 4E^0_{CL/CR}/3$, with $E^0_{CL/CR} = e^2/8\varepsilon r_{L/R}$. On the other hand, the coupling energy in the regime of strong oscillations can take different limits: When the islands are far apart, $x < 0$ and $(d-x)^2 \gg r_L r_R$, then $E_{CC} \to 0$ and the free energy given in (5) is formally equivalent to the sum of the energies of two independent islands,

$$F \simeq \frac{(V_G C_{G1} - n_L e)^2}{2e^2} E_{CL} + \frac{(V_G C_{G2} - n_R e)^2}{2e^2} E_{CR} + f(\{m_i\}, V_G^2),$$

with f being a function that does not depend on x. As they approach, E_{CC} becomes larger, with $E_{CC} \lesssim e^2/12\varepsilon r$. For $(d - x) \sim 2r$ and $C_{G1} \sim C_{G2} = C_G$, we separate the x–dependent and x–independent (g) terms,

$$F \simeq \frac{(4V_G C_G - (n_L + n_R)e)^2}{2e^2} E_{CC} + g(\{m_i\}, V_G^2),$$

which corresponds to the energy of a single island with charge $n_L + n_R$. Hence, in the large amplitude of oscillations limit, the device oscillates between the two independent islands regime and a single large island regime, giving rise to a rich structure in the response.

B. Transport in the Coulomb blockade limit

We consider the electric transport within the classical regime studied by Kulik and Shekhter [27]. Most of the single-electron effects can be explained in terms of lowest-order perturbation theory, since higher-order tunneling processes, as cotunneling, are exponentially suppressed due to the mechanical motion of the islands. The charge state is given in terms of the probabilities of having n_L excess electrons in the left island and n_R excess electrons in the right island, P_{n_L,n_R}. The tunneling processes are described in terms of transition rates within the "Orthodox" model [28], resulting in an equation of motion that describes the evolution of the charge with time. In such a picture, $\overleftrightarrow{\Gamma}^j_{n_L,n_R}$ denotes the tunneling rate across junction j in the forward or backward direction, having n_L and n_R excess electrons in either island:

$$\overleftrightarrow{\Gamma}^i_{n_L,n_R} = \frac{-\mu_i^{\rightleftarrows}}{(1 - e^{\mu_i^{\rightleftarrows}/k_B T}) e^2 R_i}. \quad (7)$$

Here, R_i is the resistance in the i-th junction, which depends exponentially on the displacement of the islands. On the flexural mode, we have

$$R_{1,3} = R^0_{1,3} e^{\frac{x}{2\lambda}}; \quad R_2 = R^0_2 e^{-\frac{x}{\lambda}} \quad (8)$$

where R^0_i is the static resistance on junction i and λ is the phenomenological tunneling length. The electrochemical potentials or addition energies, $\mu_i^{\rightleftarrows}$, denote the energy an electron needs to overcome in order to tunnel across the junction i while keeping fixed the number of electrons in junction j ($j \neq i$), $\mu_i^{\rightleftarrows}(n_L, n_R) = F(m_i \pm 1) - F(m_i)$. Figure 3 shows schematically the six different processes across the three junctions. Using the expression for the free energy (5), the electrochemical potentials for the six possible processes of Fig. 3 are

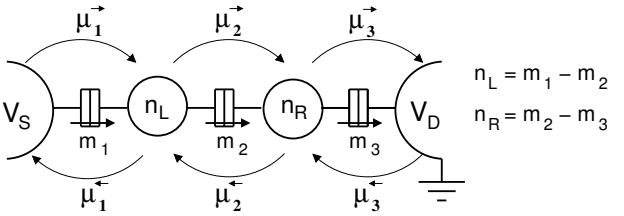

FIG. 3: *Schematic representation of the tunneling processes in a system of two islands attached to the S and D leads. Six different processes are given in terms of chemical potentials, $\mu_i^{\rightleftarrows}$, i = 1, 2, 3, as indicated in the picture.*

$$\begin{aligned}
\mu_1^{\rightleftarrows}(n_L,n_R) &= \left[\left(\frac{1}{2}\pm n_L\right)\pm\delta_L n_R\mp\frac{V_G}{|e|}\left(C_{G1}+C_{G2}\delta_L\right)\pm\frac{V(t)}{|e|}\left((C_L-C_1)-\delta_L C_2^0\right)\right]E_{CL}\\
\mu_2^{\rightleftarrows}(n_L,n_R) &= \left[1\mp n_L\mp n_R\mp\frac{V(t)}{|e|}C_1\pm\frac{V_G}{|e|}(C_{G1}-C_{G2})\right](E_{CL}-E_{CC})\\
\mu_3^{\rightleftarrows}(n_L,n_R) &= \left[\left(\frac{1}{2}\mp n_R\right)\mp\delta_R n_L\mp\frac{V_G}{|e|}\left(C_{G2}+C_{G1}\delta_R\right)\pm\frac{V(t)}{|e|}C_1\delta_R\right]E_{CR},
\end{aligned}\tag{9}$$

where we have defined $\delta_{L/R}=r_{L/R}/(d-x)$ and made the approximation $r_L\simeq r_R$ in the second equation. The master equation approach extended to multiple junctions reads

$$\begin{aligned}
\dot{P}_{n_L,n_R} &= \overrightarrow{\Gamma}^1_{n_L-1,n_R}P_{n_L-1,n_R}+\overleftarrow{\Gamma}^1_{n_L+1,n_R}P_{n_L+1,n_R}+\overrightarrow{\Gamma}^2_{n_L+1,n_R-1}P_{n_L+1,n_R-1}+\overleftarrow{\Gamma}^2_{n_L-1,n_R+1}P_{n_L-1,n_R+1}+\overrightarrow{\Gamma}^3_{n_L,n_R+1}P_{n_L,n_R+1}+\\
&+ \overleftarrow{\Gamma}^3_{n_L,n_R-1}P_{n_L,n_R-1}-\sum_{j,\rightleftarrows}\overleftrightarrow{\Gamma}^j_{n_L,n_R}P_{n_L,n_R}.
\end{aligned}\tag{10}$$

In order to understand qualitatively the charge transport in this mechanically movable device, let us focus on the charge transfer from the source to the left island in the absence of a gate voltage and in the neutral charge state, $n_L=n_R=0$. We can express the corresponding chemical potential in terms of x by using (4) in (9):

$$\mu_1^{\rightarrow}\simeq\frac{e^2(1-2x/d)}{2C_L(1+\delta_L\delta_R)}\left[1+\frac{V_S}{|V_{\rm th}^{01}|(1-x/d)}\right],$$

where we have defined the static voltage threshold $|V_{\rm th}^{01}|=|e|/2|(C_L-C_1-C_2^0\delta_L)|\sim|e|/2[C_2^0(1-\delta_L)]$ (note that the junction capacitances in the contacts are $C_1=C_L$ - C_2 - C_{G1} and $C_3=C_R$ - C_2 - C_{G2}). At zero temperature, a tunneling event requires a negative chemical potential $\mu_1^{\rightarrow}<0$, involving, in the absence of mechanical movement, a negative source voltage $V_S<0$. For a movable system, the inequality for a tunneling event to occur reads

$$|V_S|>|V_{\rm th}^{01}|(1-x/d).$$

If the voltage is in magnitude just below the threshold, say $|V_S|=|V_{\rm th}^{01}|(1-\Delta_\varepsilon)$ with $0<\Delta_\varepsilon<1$, then a negative chemical potential requires $(1-\Delta_\varepsilon)>(1-x/d)$, or $x/d>\Delta_\varepsilon>0$, involving the island separating from the left contact [recall that x is *positive* when both islands *separate* from the contacts, as in step (2) of Fig. 1(d)]. However, the resistance increases exponentially with the distance, hence suppressing the tunneling process. Small oscillations are possible due to the elastic force, but the island will not be pushed back and forth by Coulomb forces. On the contrary, beyond the threshold, say $|V_S|=V_{\rm th}^{01}(1+\Delta_\varepsilon)$, a negative potential no longer requires negative x. Tunneling of one excess electron as the island approaches the contact then becomes possible. The direction of motion of the charged cluster right after the tunneling, due to the Coulomb forces, will be away from the contact which has supplied the extra electron, and thus, we may say that the current becomes mechanically assisted. Hence, a sharp transition in the conductance of the system as the voltage increases beyond $V_{\rm th}^{01}$ is to be expected.

The same argument can be applied to the reverse jump, from the left island to the 'S' electrode,

$$\mu_1^{\leftarrow}\simeq\frac{e^2(1-2x/d)}{2C_L(1+\delta_L\delta_R)}\left[1-\frac{V_S}{|V_{\rm th}^{01}|(1-x/d)}\right].$$

A negative chemical potential for the static island $\mu_1^{\leftarrow}<0$ requires now $V_S>0$ and $|V_S|>|V_{\rm th}^{01}|$. If the voltage is just below the threshold, $V_{\rm th}^{01}(1-\Delta_\varepsilon)$, a negative chemical potential involves as well $x/d>\Delta_\varepsilon$, a process then exponentially suppressed.

It is easy to see that a similar situation occurs with the transport involving the right island and the right contact, since we have, by examining Eq. (9):

$$\mu_i^{\rightleftarrows}\simeq\frac{e^2(1-2x/d)}{2C_{\alpha_i}(1+\delta_L\delta_R)}\left[1\pm\frac{V_S}{V_{\rm th}^{0i}(1-x/d)}\right],$$

with i = 1, 3, $\alpha_1=L$, $\alpha_3=R$ and $V_{\rm th}^{03}=|e|\delta_R/2C_1$. Again, at zero temperature, a charge transfer from the right island to the right contact would require the island to separate from the contact when the voltage is just below the threshold $V_{\rm th}^{03}$. The x dependency for $\mu_2^{\rightleftarrows}$ is not as important as in the other four processes, but naturally, the tunneling is favored as the islands approach each other, $x>0$.

We compute the current in the stationary limit, *i.e.*, when the transient solutions become negligible in the oscillations,

$$I_{\rm DC}\sim -e\sum_{n_\alpha,n_\beta}P_{n_\alpha,n_\beta}\left[\overrightarrow{\Gamma}^\alpha_{n_\alpha,n_\beta}-\overleftarrow{\Gamma}^\alpha_{n_\alpha,n_\beta}\right],\tag{11}$$

where the non-equilibrium probability distribution P_{n_α,n_β} is a stationary solution of the kinetic equation, (10). To perform our calculations, we used materials parameters mostly based on typical experimental values; see Table I. Figure 4 shows

TABLE I: *Materials parameters used in this work. (PC = personal communication with Prof. Dr. Robert H. Blick, AE = authors estimation).*

Parameter	Value	Units	Ref. #
β_1	6.25	μm^{-1}	[25]
E	150	GPa	[26] & AE
γ	.05	--	PC
R_2^0	40	$G\Omega$	[3]
$R_{1,3}^0$	20	$G\Omega$	[3]
C_2^0	2	aF	[3]
$C_{1,3}^0$	4	aF	[3]
h	250	nm	[2], [3]
r_R	32	nm	[3]
r_L	28	nm	[3]
d	45	nm	[3]
r_0	7.5	nm	AE
L	150	nm	[3]
λ	5	nm	AE
m	2×10^{-18}	Kg	[2], [3]
ω_0	250	MHz	[2]
ε	10^{-2}	--	AE

the numerical results of the absolute value of the normalized current $|I_{\rm dc}|$ using Eqs. (10) and (11), in units of $I_{\rm th}$, the current at the threshold bias, $V_{\rm th}$. The Coulomb blockade diamonds are apparent, a result of the discrete nature of the electronic charge [3, 30].

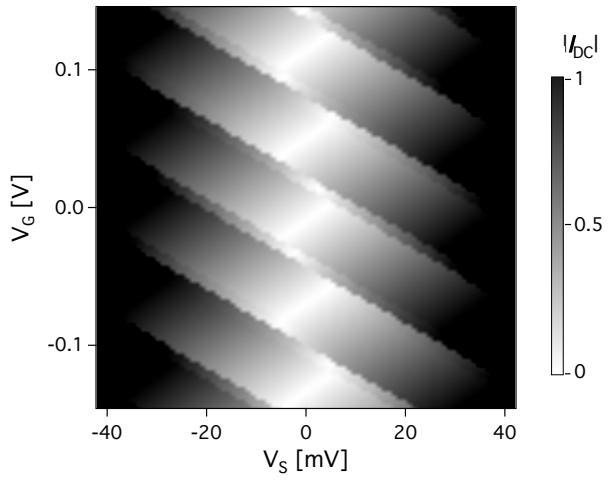

FIG. 4: *Contour plot of the absolute value of the direct current $|I_{\rm dc}|$ as a function of V_S and V_G. The radii of the nanoislands were set to $r_L = 28$ nm and $r_R = 31$ nm. Coulomb blockade diamonds are apparent, even at room temperature.*

We now consider a rf signal superimposed to the dc one, $V_S = V(t)$. The electron transfer between the islands to the right direction will occur *in phase* with the signal, and the electron transfer to the right direction between a contact and its nearest island will occur *out of phase* with the signal (see Fig. 5). The sequence of electronic transport is schematically depicted in Fig. 5: The sign of the current is determined now by the initial conditions, occurring left to right in Fig. 5(a) and right to left in Fig. 5(b).

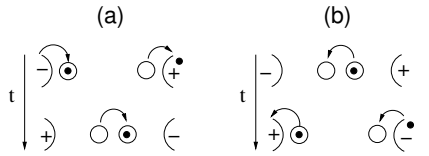

FIG. 5: *Electronic transport through a double pendula structure. The direct current is to the right (a) [left, (b)] direction if the metallic grains approach the contacts (each other) when the applied bias is negative. Electron transfer between the islands to the right (left) direction occurs in (out of) phase with the signal, as depicted in bottom of (a) [top of (b)].*

If the frequency of the rf signal is close to the natural frequency of resonance ω_0, the oscillatory motion can assist the conductance by significant displacements of the island. The oscillatory regime in the frame of nonlinear dynamics is studied in the subsequent sections.

IV. ELECTRO-MECHANICAL DYNAMICS: COUPLED MODE AND PARAMETRIC ELECTRONICS

As we noted before, the capacitances and the resistances depend on the displacements of the islands, hence affecting the chemical potentials and the tunneling processes, respectively. We want to take into account explicitly the oscillatory movement of the islands into the electrostatics. To do so, we first express the free energy in terms of E_{Ci} defined in Eq. (6):

$$\begin{aligned} F(x;\{m_i\}) &= E_{CL}(x)\eta_L(\{m_i\}) + E_{CR}(x)\eta_R(\{m_i\}) \\ &+ E_{CC}(x)\eta_C(\{m_i\}), \end{aligned} \tag{12}$$

where we have defined the set of variables η as:

$$\begin{aligned} \eta_L &= \frac{n_L}{2} - \frac{m_1}{|e|}\left[V_G C_{G1} + V_S(C_L - C_1)\right] - \frac{m_2}{|e|}\left[V_S C_1\right] \\ \eta_R &= \frac{n_R}{2} + \frac{m_3}{|e|}\left(V_G C_{G2}\right) \\ \eta_C &= n_L n_R - \frac{m_1}{|e|}\left[V_G C_{G2} + V_S C_2^0\right] + \frac{m_2}{|e|}\left(V_S C_1\right) + \\ &+ \frac{m_3}{|e|}\left(V_G C_{G1} + V_S C_1\right) \end{aligned}$$

Next, we expand E_{Ci} in terms of the relative displacement $x_d = x/d$ (note that $x_d < 1$):

$$\begin{aligned} E_{CL/R} &\simeq \frac{e^2}{8\varepsilon r_{L/R}(1-\delta_r)}\left[1 + \frac{2\delta_r}{1-\delta_r}x_d + \frac{3\delta_r+\delta_r^2}{(1-\delta_r)^2}x_d^2 + \ldots\right] \\ E_{CC} &\simeq \frac{e^2}{8\varepsilon d(1-\delta_r)}\left[1 - \frac{1+\delta_r}{1-\delta_r}x_d + \frac{1+3\delta_r}{(1-\delta_r)^2}x_d^2 + \ldots\right], \end{aligned} \tag{13}$$

where $\delta_r = r_L r_R/d^2 \ll 1$. We include the electrostatic force in the coupled harmonic oscillators by adding the term $F(n_L,n_R;x)$ to the Lagrangian, $\mathcal{L} = m\dot{x}^2/2 - kx^2/2 - F(n_1,n_2;x)$. Using the leading terms in δ_r for the derivative of Eq. (13), we have:

$$-\frac{\partial F}{\partial x} \simeq -\frac{e^2}{8\varepsilon d}\left\{\left(\frac{\eta_L}{r_L}+\frac{\eta_R}{r_R}\right)\delta_r\sum_{n=1}^{\infty}\frac{n(n+1)x_d^{n-1}}{(1-\delta_r)^n}+ +\frac{\eta_C}{d}\sum_{n=1}^{\infty}\frac{nx_d^{n-1}}{(1-\delta_r)^n}\right\} \quad (14)$$

The Lagrange's equation of motion for the relative coordinate x now reads:

$$m\ddot{x}+m\gamma\dot{x}+kx = -\frac{\partial F}{\partial x} \rightarrow m\ddot{x}+m\gamma\dot{x}+(k+\Delta_k)x = -\Delta_F \quad (15)$$

where we have introduced the damping force, $F_\gamma = m\gamma\dot{x}$ and defined

$$\Delta_k = \frac{e^2}{4\varepsilon d^2(1-\delta_r)^2}\left[3\delta_r\left(\frac{\eta_L}{r_L}+\frac{\eta_R}{r_R}\right)+\frac{\eta_C}{d}\right];$$
$$\Delta_F = -\frac{e^2}{8\varepsilon d(1-\delta_r)}\left[2\delta_r\left(\frac{\eta_L}{r_L}+\frac{\eta_R}{r_R}\right)+\frac{\eta_C}{d}\right].$$

Equation (15) is known as a damped Mathieu equation [31]. It includes a standard harmonic oscillator driving term, and a *parametric modulation* term, which is a variable spring constant, Δ_k. We note that Δ_k and Δ_F depend in general on time, as the shuttle oscillates causing a charge transfer. A rough estimation for a realistic system gives $\Delta_F \simeq 0.2-1$ pN. $\eta_{L,R,C}$ depend on the number of excess electrons on each of the islands, $n_{L/R}$. As we will see below, in the shuttling regime, $n_{L/R}$ is a function that oscillates with time, as the mechanical movement of the islands assist the electronic transport through the device. Thus, Δ_k and Δ_F are time-dependent functions, and Eq. (15) is a modified Mathieu equation, which can be treated numerically [32]. In the following subsections, we consider two different limits to understand the dynamics of the system.

A. Small oscillations limit in the linear regime

We consider first the small oscillations within the classical circuit limit. In the linear adiabatic regime, the charge balance in the islands follows the excitation given by the applied voltage, $V(t)$. From classical circuit theory, we have that the applied voltage equals to the sum of the voltages that drop on each junction, and the net current through each of the junctions is the same,

$$V_{SD} = V(t) = \sum_{i=1}^{3}\frac{q_i}{C_i}; \quad \frac{q_i}{R_iC_i} = \frac{q_j}{R_jC_j}. \quad (16)$$

We can solve the above system of equations for $q_i = -|e|m_i$ and get the charge on each island, $Q_i = -|e|n_i$: $Q_L = q_1 - q_2$; $Q_R = q_2 = q_3$. When the flexural modes of the nanopillars are excited, the mutual capacitance and the resistances become sensitive to the displacements, x_L and x_R. In a flexural mode in which the center of mass is at rest ($X_0 = 0$), as in Fig. 1(d), the resistances are given by (8). The mutual capacitance C_2 determining the coupling of the metallic islands depends as well in their separation, whereas $C_{1,3}$ can be considered as constant,

$$C_{1,3} \simeq C_{1,3}^0; \quad C_2(x) = \frac{C_2^0}{1-x/d}.$$

Further, we will make the approximation that $R_i^0C_i^0$ is a constant, but the resistance R_2 is twice the resistances $R_{1,3}$. We set $R_1^0 = R_3^0 = R_2^0/2$ and $C_1^0 = C_3^0 = 2C_2^0 = C$, consistent with previous results [3]. From now on, we express the relative coordinate in units of λ, $x \equiv x/\lambda$. Using (16) we get

$$q_2 = \frac{CV(t)}{2(1-x/d)(1+e^{3x/2})}; \quad q_1 = -q_3 = \frac{CV(t)e^{3x/2}}{2(1+e^{3x/2})},$$

giving a compact expression for $Q_L = -Q_R$,

$$Q_L \simeq \frac{CV}{2}\left[\tanh\frac{3x}{4}-\frac{x}{d}e^{3x/4}\right] \simeq \frac{3CV}{4}\left[x-\frac{2}{d}x^2-\frac{3}{16}x^3\right]. \quad (17)$$

At lowest order in x, we have a symmetric system whose islands have no net charge at $x = 0$. Then, for $x < 0$ (so the pillars are away from each other, getting close to the contacts), a net charge with negative sign is induced in island L and a positive one in R. Note that the potential is, by convention, negative on the left and positive on the right contact. Reversing the potential V will cause a change of sign in Q_L and Q_R, as expected. The two nonlinear terms on the right break the left-right symmetry of the system.

The dynamics of the nanopillars will consist of a set of oscillators experiencing the electric field, $V(t)/L$. We follow the approach given by Ahn *et al.* [22] to investigate the electrodynamics of the system. We find the equations of motion of the relative coordinate x by setting $m = m_R \simeq m_L$ and substituting Eq. (17) into Eq. (15),

$$\ddot{x}+\frac{\gamma}{\omega_0}\dot{x}+x = -\alpha\sin^2\omega\tau\left[x-\frac{2\lambda}{d}x^2-\frac{3}{16}x^3\right].$$

Here $\alpha = 3CV_0^2/4Lm\lambda\omega_0^2$, a dimensionless forcing parameter which account for the ratio of the electric ($F_e \sim CV_0^2/L$) and mechanical forces ($F_m \sim m\lambda\omega_0^2 = k\lambda$). We note that for a typical Si nanopillar, $F_m \sim 50-60$ pN and $F_e \sim 1-5$pN. We have also rescaled the time, $\tau = \omega_0 t$. ω is the frequency of the excitation, expressed in units of ω_0. This is a non-linear equation that corresponds to a forced and damped oscillator, where the forcing terms depend on the coordinate itself. At first order in x, we obtain a modified Mathieu equation, which gives instability regions when the excitation is strong enough. We are, however, interested also in the weak excitation regime, in which the non-linear terms and non-linear effects such as Coulomb blockade could play a critical role.

Following the Poincaré-Lindstedt method, we parametrize the damping and the forcing using a small arbitrary ε ($\varepsilon \ll 1$),

$\gamma \sim \varepsilon\gamma_1$, $\alpha \sim \varepsilon\alpha_1$,

$$\ddot{x} + x + \varepsilon\left(\gamma_1\dot{x} + \alpha_1 \sin^2\omega\tau\left[x - \frac{2\lambda}{d}x^2 - \frac{3}{16}x^3\right]\right) = 0. \quad (18)$$

Thus, we can consider two different time scales, the "stretched" time, $z = \omega\tau$, and the "slow" time, $\eta = \varepsilon\tau$. The time derivatives are now expressed in terms of these new times as

$$\dot{x} = \omega\frac{\partial x}{\partial z} + \varepsilon\frac{\partial x}{\partial \eta}; \quad \ddot{x} = \omega^2\frac{\partial^2 x}{\partial z^2} + 2\varepsilon\omega\frac{\partial^2 x}{\partial\eta\partial z} + \varepsilon^2\frac{\partial^2 x}{\partial\eta^2}. \quad (19)$$

We expand x in terms of ε,

$$x(z,\eta) \simeq x_0 + \varepsilon x_1 + \ldots \quad (20)$$

and, likewise, seek for solutions that correspond to harmonics of the natural frequency ω_0:

$$\omega \simeq p + \varepsilon\delta_\omega + \ldots, \quad (21)$$

where p is an integer or fractional number and, finally, substitute (19), (20), and (21) into (18), neglecting terms of $O(\varepsilon^2)$, which gives, after collecting terms at lowest order in ε,

$$\frac{1}{p^2}\frac{\partial^2 x_0}{\partial z^2} + x_0 = 0$$

giving a general solution for x_0,

$$x_0(z,\eta) = A(\eta)\cos\frac{z}{p} + B(\eta)\sin\frac{z}{p}. \quad (22)$$

The constants of integration, A and B are functions of the "slow" time η. At first order in ε we get:

$$\begin{aligned}\frac{\partial^2 x_1}{\partial z^2} + x_1 &= -2\frac{\partial^2 x_0}{\partial z\partial\eta} - 2\delta_\omega\frac{\partial^2 x_0}{\partial z^2} - \gamma_1\frac{\partial x_0}{\partial z} - \\ &- \alpha_1(1-\cos 2z)\left[x_0 - \frac{2\lambda x_0^2}{d} - \frac{3x_0^3}{16}\right]. \quad (23)\end{aligned}$$

Without loss of generality, we may ask that x_1 satisfies $\ddot{x}_1 + x_1 = 0$. We substitute the general solution (22) for $p = 1$ into the above expression and arrange terms in $\sin z$ and $\cos z$ (see Appendix B 1) to get:

$$\begin{aligned}2\frac{\mathrm{d}A}{\mathrm{d}\eta} &= -\gamma_1 A - \left(2\delta_\omega - \frac{3\alpha_1}{2}\right)B - \frac{3\alpha_1}{64}B(3A^2+5B^2); \\ 2\frac{\mathrm{d}B}{\mathrm{d}\eta} &= -\gamma_1 B + \left(2\delta_\omega - \frac{\alpha_1}{2}\right)A + \frac{3\alpha_1}{64}A(A^2+3B^2).\end{aligned} \quad (24)$$

Note that equilibrium points of (24) correspond to periodic solutions of our forced oscillator, and the norm of the solutions is conserved, *i.e.*: $A^2 + B^2 = x_0^2 + \dot{x}_0^2$.

If a dc signal is superimposed, $V(t) = V_0(\sin\omega\tau + \beta)$ with $\beta = V_{dc}/V_0$, Eq. (18) will now read

$$\varepsilon\left\{\gamma_1\dot{x} + \alpha_1[\sin^2\omega\tau + 2\beta\sin\omega\tau + \beta^2]\left[x - \frac{2\lambda}{d}x^2 - \frac{3}{16}x^3\right]\right\} + \ddot{x} + x = 0.$$

Proceeding in the same manner as before, we find six extra terms (terms in β or β^2). We consider the stretched and slow time, and expand x and ω in terms of ε, to get, for the $p = 1$ case (see Appendix B 2):

$$\begin{aligned}\frac{\mathrm{d}A}{\mathrm{d}\eta} &= -\gamma_1 A - \left(\delta_\omega - \frac{3\alpha_1}{4} - \alpha_1\beta^2\right)B - \frac{\alpha_1\beta\lambda}{d}(A^2+3B^2) - \frac{27\alpha_1\beta^2}{64}B(A^2+B^2) - \frac{3\alpha_1}{128}B(3A^2+5B^2) \\ \frac{\mathrm{d}B}{\mathrm{d}\eta} &= -\gamma_1 B + \left(\delta_\omega - \frac{\alpha_1}{4} - \alpha_1\beta^2\right)A + \frac{2\alpha_1\beta\lambda}{d}AB + \frac{27\alpha_1\beta^2}{64}A(A^2+B^2) + \frac{3\alpha_1}{128}A(A^2+3B^2)\end{aligned} \quad (25)$$

and for the p = ''any" case, (see Appendix B 3):

$$
\begin{aligned}
2\frac{dA}{d\eta} &= -A(\gamma_1-\beta\alpha_1\delta_{p,2}) - B\left(\frac{2\delta_\omega}{p}-\frac{\alpha_1}{4}(2+\delta_{p,1}+4\beta^2)\right) + AB\frac{\alpha_1\lambda}{8d}\delta_{p,3/2} + (A^2-B^2)\frac{\beta\alpha_1\lambda}{4d}\delta_{p,3} \\
&\quad -\frac{3\alpha_1}{256}\left[B(A^2+B^2)(6+12\beta^2+3\delta_{p,1}) + B(3A^2-B^2)\delta_{p,2} + 6A(A^2+B^2)\delta_{p,2} + 2A(A^2-3B^2)\delta_{p,4}\right] \\
2\frac{dB}{d\eta} &= -B(\gamma_1+\beta\alpha_1\delta_{p,2}) + A\left(\frac{2\delta_\omega}{p}-\frac{\alpha_1}{4}(2-\delta_{p,1}+4\beta^2)\right) + (A^2-B^2)\frac{\alpha_1\lambda}{16d}\delta_{p,3/2} - AB\frac{\beta\alpha_1\lambda}{2d}\delta_{p,3} \\
&\quad +\frac{3\alpha_1}{256}\left[A(A^2+B^2)(6+12\beta^2-3\delta_{p,1}) - A(A^2-3B^2)\delta_{p,2} + 6B(A^2+B^2)\delta_{p,2} + 2B(3A^2-B^2)\delta_{p,4}\right]
\end{aligned}
\tag{26}
$$

The stability of the solutions of the equation above can be investigated using numerical methods [32].

In order to understand qualitatively the electromechanical motion scenario, we consider, first, the case $p = 1$ and $\beta = 0$, where Eq. (25) reads ($\dot{A} \equiv dA/d\eta$)

$$
\begin{aligned}
2\dot{A} &= -\gamma_1 A - (\gamma_2-\gamma_3)B - \gamma_4 B(3A^2+5B^2) \\
2\dot{B} &= -\gamma_1 B + (\gamma_2+\gamma_3)A + \gamma_4 A(A^2+3B^2)
\end{aligned}
$$

where we have defined $\gamma_2 = 2\delta_\omega - \alpha_1$, $\gamma_3 = \alpha_1/2$, and $\gamma_4 = 3\alpha_1/64$. It is easy to see that the transition curves for the stability of the trivial solution are $\gamma_2 = \pm\gamma_3$, or $\alpha_1 = 4\delta_\omega, 4\delta_\omega/3$. Along this curves (broken lines of Fig. 6) the stability of $r_0 = 0$ changes. To gain in simplicity, we transform to polar coordinates in the A-B phase plane, by setting $A = r_0\cos\varphi$ and $B = r_0\sin\varphi$. The amplitude $r_0^2 = A^2+B^2$ and the phase $\varphi = \arctan B/A$ now satisfies:

$$
\begin{aligned}
2\dot{r}_0 &= -\gamma_1 r_0 + r_0\sin 2\varphi(\gamma_3 - \gamma_4 r_0^2) \\
2\dot{\varphi} &= \gamma_2 + \gamma_3\cos 2\varphi + \gamma_4 r_0^2(3-2\cos 2\varphi)
\end{aligned}
\tag{27}
$$

We seek equilibria of the "slow flow" (27). A solution in which r_0 and φ are constant represents a periodic motion of the nonlinear Mathieu equation, which has the frequency of the forcing function. Such equilibria satisfy $\dot{r}_0 = \dot{\varphi} = 0$. Ignoring the trivial solution $r_0 = 0$, the first equation of (27) with $\dot{r}_0 = 0$ requires

$$
\sin 2\varphi = \frac{\gamma_1}{\gamma_3 - \gamma_4 r_0^2}.
$$

In the absence of damping $\gamma_1 \sim 0$, find equilibria at $\varphi = 0, \pi/2, \pi, 3\pi/2$. The second equation of (27) with $\dot{\varphi} = 0$ then implies

$$
r_0^2 = -\frac{\gamma_2+\gamma_3\cos 2\varphi}{\gamma_4(3-2\cos 2\varphi)} = -\frac{\gamma_2 \mp \gamma_3}{\gamma_4(3\mp 2)}.
$$

For a nontrivial real solution, $r_0^2 > 0$. In the case of $\varphi = 0$ or π, $\cos 2\varphi = 1$ and nontrivial equilibria require $-\gamma_3 - \gamma_2 > 0$ or $4\delta_\omega < \alpha_1$. On the other hand, for $\varphi = \pi/2$ or $3\pi/2$, $\cos 2\varphi = -1$ and nontrivial equilibria require $\gamma_3 - \gamma_2 > 0$ or $4\delta_\omega < 3\alpha_1$. Since $\delta_\omega = \alpha_1/4$ and $\delta_\omega = 3\alpha_1/4$ correspond to transition curves for the stability of the trivial solution, bifurcations occur as we cross the transition curves in the δ_ω-α_1 plane (see Fig. 6). Keeping α_1 fixed as we shift δ_ω from the right across the right transition curve, the trivial solution $r_0 = 0$ becomes unstable and simultaneously two branches of stable solutions are born, one with $\varphi \sim \pi/2$ and the other with $\varphi \sim 3\pi/2$. This motion grows in amplitude as δ_ω continues to decrease. When the left transition curve is crossed, the trivial solution becomes stable again. This scenario can be pictured as involving two pitchfork bifurcations, as depicted in Fig. 6.

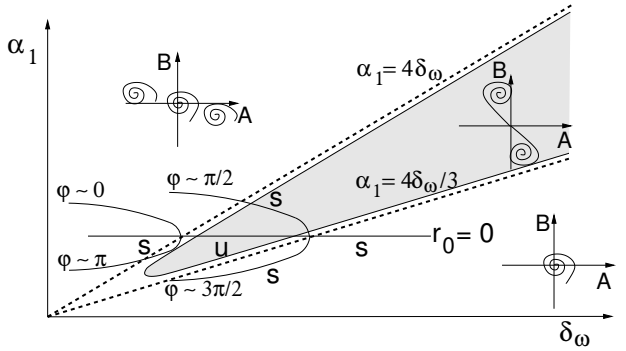

FIG. 6: *Schematic representation of the p = 1 tongue in the parameter space spanned by δ_ω and α_1. Between the transition curves (broken lines), the trivial solution is unstable and two stable solutions are born, φ = 0, π (solid curves). The insets depict phase portraits in the A-B plane: below the lower transition curve, only the trivial solution exists. In between both transition curves, the trivial solution is unstable, and another two solutions are born. Above the second transition curve, r_0 = 0 is stable again, and the other two solutions become unstable.*

A finite damping γ_1 shifts slightly the position of the stable equilibria in the A-B plane, which become stable spirals, as represented in the insets of Fig. 6. The damping also "shrinks" the region of instability (shaded area of Fig. 6), lifting it away from the origin in the parameter space.

In the classical limit, we can have an idea of the resulting direct current through the system. The time-average direct current is obtained by integrating over a period the current across one of the three junctions of Fig. 2,

$$
I_{\rm dc} = \frac{\omega}{4\pi R}\int_{t_0}^{t_0+T}\frac{V(t)e^x}{1+e^{3x/2}}. \tag{28}
$$

We study (28) in terms of the coefficients r_0 and φ, $x = r_0\cos(\omega t - \varphi)$. We find that the absolute value of the direct current reaches a maximum when $\varphi = 0, \pi$ and $r_0 = 2$.

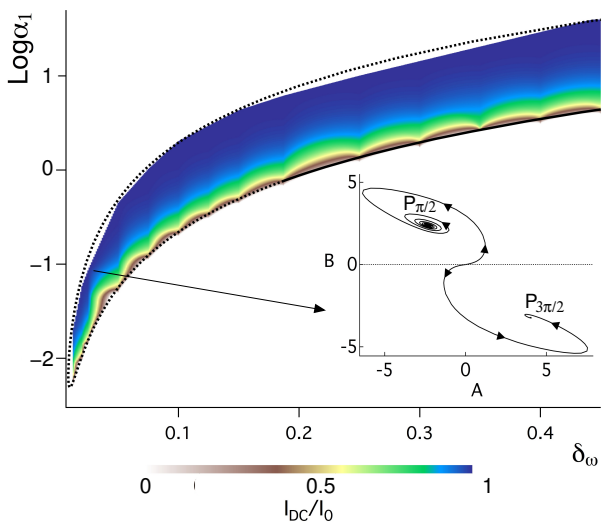

FIG. 7: *(Color online) Contour plot of the direct current I_{dc} as a function of α_1 and δ_ω in the first tongue, $p = 1$. The inset shows a phase portrait in the A-B plane: inside the tongue, the origin is unstable, and two stable solutions are found, $P_{\pi/2}$ and $P_{3\pi/2}$.*

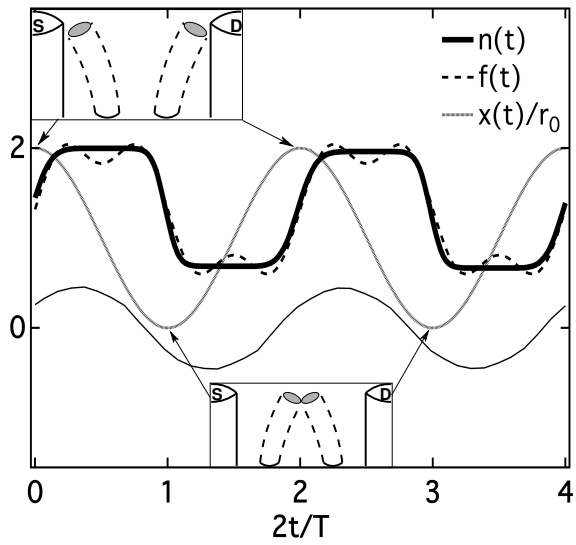

FIG. 8: *Time evolution of $n(t) = n_l - n_R$ in the stationary limit for low (thin solid curve) and high bias (thick solid curve). In the high bias regime, $n(t)$ can be approximated by a square wave.*

Figure 7 shows numerical results of I_{dc} in the $p = 1$ tongue, where α_1 is in log scale. Inside the tongue, the trivial solution is unstable, and two stable solutions appear at $P_{\pi/2}$ and $P_{3\pi/2}$ in the *A*-*B* plane (see inset). The trajectories stay either in the upper or lower semiplane; thus, the initial conditions determine the point of stability: If $\varphi(0) > 0$ (< 0), then the phase portrait in the *A*-*B* plane reaches $P_{\pi/2}$ ($P_{3\pi/2}$) and the electron transport is right to left (left to right), using the convention of Fig. 5. At these points, the nanopillars are oscillating with the natural frequency of the oscillations, mechanically assisting the electronic transport.

B. Oscillations in the shuttling regime

So far we have studied the limit when the charge in the metallic islands is given by Eq. (17), *i.e.*, the charge on the islands $Q_{L,R}$ changes continuously, following the excitation $V(t)$. As the size of the metallic islands shrinks, however, we may reach the discrete limit, where single-electron effects such as Coulomb blockade become important. In the Coulomb blockade limit, as we have seen in Sec. III B, an extra electron can only be added to the island if enough energy is provided by the external sources to overcome the Coulomb repulsion between the electrons. The equation of motion for the relative coordinate reads:

$$\ddot{x} + \gamma\dot{x} + x = \frac{eV(t)}{kL\lambda} n(t), \tag{29}$$

where $n(t) = n_L(t) - n_R(t)$.

The evolution of the probabilities of having n_L excess electrons on the left island and n_R on the right island is given by Eq. (10) , which is solved by direct integration. Figure 8 shows numerical results of the function $n(t)$ obtained solving simultaneously the master equation [Eqs. (7)-(10)] and the dynamic equation, [Eq. 29] in the stationary regime. In the low bias limit, $n(t)$ is a sinusoidal function that follows the excitation $V(t)$ (thin solid curve of Fig. 8). The charge has only a small probability to be transferred across the device, following the bias. However, after some critical bias, the charge transfer occurs mostly at the points of maximal deflection, commonly termed as shuttling regime. We obtain numerically $n(t)$, resulting a square wave correlated with the excitation $V(t)$ (thick solid curve of Fig. 8),

$$n(t) \simeq n_{\rm av} + 4n_0(\cos\omega_0 t - \cos 3\omega_0 t)/\pi, \tag{30}$$

where $n_{\rm av}$ and n_0 are obtained after averaging over a large number of simulations and depend on the input parameters. We note that the charge transfer occurs in the points of maximal deflection during an effective contact time, in accordance with Weiss *et al.* [29].

Inserting the expression (30) into (29), we aim, as before, for oscillatory solutions, $x_0 \simeq A(\eta)\cos z/p + B(\eta)\sin z/p$, bearing in mind the following linearized equations for the coefficients A and B (see Appendix B 4):

$$\begin{aligned} 2\frac{dA}{d\eta} &= -\gamma_1 A - \frac{2\delta_\omega}{p}B + n_{\rm av}\alpha_1'\delta_{p,1} + n_0\frac{\alpha_1'}{6}(2\delta_{p,2} - \delta_{p,4}) \\ 2\frac{dB}{d\eta} &= -\gamma_1 B + \frac{2\delta_\omega}{p}A + \alpha_1'\beta n_0, \end{aligned} \tag{31}$$

where we have defined $\alpha' = eV_0/Lk\lambda$ and $\alpha_1' = \varepsilon\alpha'$. As before, α' can be viewed as the ratio between the electrical and mechanical forces. We find the equilibrium or stable points by solving Eq. (31) with $\dot{A} = \dot{B} = 0$. In the absence of $V_{\rm dc}$ ($\beta = 0$), non-trivial stable points are found only around subharmonics

with p = 1, 2, or 4,

$$\begin{aligned}(A_{\rm eq},B_{\rm eq})_{p=1} &= \frac{\alpha' n_{\rm av}}{\gamma_1^2+4\delta_\omega^2}(\gamma_1,2\delta_\omega)\\ (A_{\rm eq},B_{\rm eq})_{p=2} &= \frac{\alpha' n_0}{3(\gamma_1^2+\delta_\omega)^2}(\gamma_1,\delta_\omega)\\ (A_{\rm eq},B_{\rm eq})_{p=4} &= \frac{\alpha' n_0}{6(\gamma_1^2+(\delta_\omega/2)^2)}\left(\gamma_1,\frac{\delta_\omega}{2}\right)\end{aligned} \qquad (32)$$

In contrast, under a finite dc bias, nontrivial stable points are found for *any* frequency at

$$(A_{\rm eq},B_{\rm eq})_p = \frac{\alpha\beta n_0}{\gamma_1^2+(2\delta_\omega/p)^2}\left(\frac{2\delta_\omega}{p},-\gamma_1\right). \qquad (33)$$

We stress that this result is valid in the limit of large oscillations. To estimate the range of validity of Eqs. (32) and (33), we consider the limit of small oscillations, for which the charge on the islands "follows" the mechanical motion, with an amplitude proportional to the amplitude of the oscillations, $r_0=\sqrt{A^2+B^2}$,

$$n(t)\simeq a_n r_0 \sin\omega_0 t.$$

In this limit, Eq. (31), in polar coordinates and for $\beta\neq 0$ and $p\neq 2$ reads

$$\dot{r_0^2} = -\frac{1}{\gamma_1}r_0^2+\alpha_1'\beta a_n A r_0,$$

We find a change in the stability of $r_0=0$ when the forcing parameter exceeds a threshold, $\alpha_1'\beta a_n>\alpha_{\rm th}'$, with

$$\alpha_{\rm th}'=\sqrt{\gamma_1^2+\delta_\omega^2}.$$

r_0 changes from a stable to an unstable spiral as the forcing is increased beyond $\alpha_{\rm th}'/(\beta a_n)$. In this situation, the amplitude of the oscillations could reach the Fowler-Nordheim tunneling limit [33], with a subsequent enhancement of the direct current due to field emission, marking the limit of validity of the present model.

C. Dissipated and absorbed power by the oscillators

We focus now on the dissipated and absorbed power by the shuttles. According to Eq. (29), the (unitless) power loss per unit cycle of duration T will be given by

$$\langle W_{\rm dis}\rangle = \gamma\langle\dot{x}^2\rangle = \frac{1}{2}\gamma r_0^2.$$

Similarly, we can obtain the absorbed power per unit cycle by averaging over a period the pumped energy of the electrostatic force given by the last term of Eq. (29,

$$\langle W_{\rm a}\rangle \simeq \left\langle \alpha' n(t)\dot{x}(t)(\sin\omega t+\beta)\right\rangle.$$

Due to the correlation between charge fluctuations $n(t)$ and the velocity of the nanopillars, $\dot{x}(t)$, a positive amount of energy may be pumped into the system. For instance, for the finite dc bias cases, the amount of energy pumped into the system per cycle in steady state [at $(A_{\rm eq}, B_{\rm eq})_p$] is

$$\langle W_{\rm a}\rangle = \frac{r_0\alpha'}{12}\left[6\beta n_0\cos\varphi+(6n_{\rm av}\delta_{p,1}+2n_0\delta_{p,2}-n_0\delta_{p,4})\sin\varphi\right].$$

If this amount is larger than the dissipated power, $\langle W_{\rm a}\rangle \gtrsim \langle W_{\rm dis}\rangle$, self-sustained oscillations are expected. This may occur when $\max\{\alpha' n_{{\rm av},0},\alpha' n_0\beta\}\gtrsim\gamma r_0$, with the appropriate phase φ. In particular, for the branch with $\varphi\sim 0$, the condition reads $\alpha'\beta n_0>\gamma r_0$. In other words, self-sustained oscillations may occur for a wide range of frequencies if the appropriate values of α and β are met.

V. CONCLUSIONS

We have theoretically studied a coupled shuttle consisting of two oscillating nanoislands connected in series between two contacts. We express the chemical potentials in terms of the relative distance of the islands, $\mu_i^{\leftrightarrows}[x(t)]$, and numerically integrate the master equation to obtain the direct current through the system. Under a dc bias, Coulomb blockade diamonds were obtained. Adding an rf signal, we analyze the response within the context of nonlinear dynamics. We study qualitatively and quantitatively the structure of the mode-locked tongues in the parameter space. Parametric instabilities are observed in a range of applied voltages and frequencies, where resulting small mechanical oscillations are amplified. In this instability region, an rf signal can be exploited to parametrically amplify the response to a gate excitation. Hence, we propose a practical scheme for direct detection of instabilities in the mechanical motion of nanoscale objects.

Acknowledgments

We are grateful to R. H. Blick and C. Kim for enlightening discussions. This work was supported by the Spanish Ministry of Education, program SB2009-0071.

Appendix A: Free energy of a double coupled metallic island

In this appendix we derive the free energy of a double metallic grain system. In general, for a system of N conductors, the total charge on each node j is the sum of the charges on all of the capacitors connected to node j, $-en_j = -e\sum_k m_k = \sum_k C_k(V_j - V_k)$, where V_j is the electrostatic potential of node j and ground is defined to be at zero potential. The charges on the nodes are linear functions of the potential of the nodes, $\vec{Q} = \tilde{C}\vec{V}$, where $\tilde{C}$ is the capacitance matrix. For

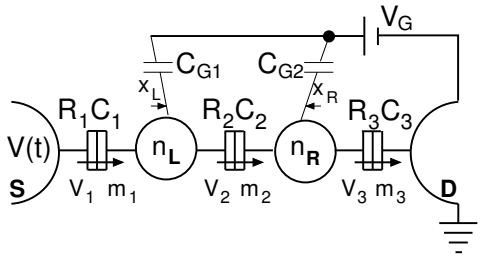

FIG. 9: *A schematic picture of the double-island structure with the voltage sources and various capacities in the system. The three junctions are characterized by m_j and V_j, j = 1, 2, 3. The islands are coupled to each other, with a mutual capacitance C_2, as well as to a gate voltage, V_G with capacitances C_{G1} and C_{G2}, respectively. Also, they are coupled to the source-drain leads, with capacitances C_1 and C_3.*

the system depicted in Fig. 9, we have:

$$\begin{aligned} Q_L &= C_2(V_L - V_R) + C_1(V_L - V_S) + C_{G1}(V_L - V_G) \\ Q_R &= C_2(V_R - V_L) + C_3(V_R - V_D) + C_{G2}(V_R - V_G), \end{aligned} \quad \text{(A1)}$$

where $Q_i^{\rm bg}$ is the "residual" charge in dot i when all potentials are grounded. We can write this in the form $\vec{Q} + \vec{\alpha} = \tilde{C}\vec{V}$, with $\tilde{C}$ being the capacitance matrix,

$$\begin{pmatrix} Q_L + C_1V_S + C_{G1}V_G \\ Q_R + C_3V_D + C_{G2}V_G \end{pmatrix} = \begin{pmatrix} C_L & -C_2 \\ -C_2 & C_R \end{pmatrix} \begin{pmatrix} V_L \\ V_R \end{pmatrix},$$

where $C_L = C_1 + C_2 + C_{G1}$ and $C_R = C_3 + C_2 + C_{G2}$. We can thus set our node voltages in terms of the capacitances,

$$\begin{pmatrix} V_L \\ V_R \end{pmatrix} = \frac{1}{C_LC_R - C_2^2} \begin{pmatrix} C_R & C_2 \\ C_2 & C_L \end{pmatrix} \begin{pmatrix} Q_L + C_1V_S + C_{G1}V_G \\ Q_R + C_3V_D + C_{G2}V_G \end{pmatrix}.$$

The electrostatic energy of the system can now be calculated, $U = \vec{V}\tilde{C}\vec{V}/2$, with $V_S = V_D = V_G = 0$,

$$U(n_L, n_R) = \frac{e^2}{C_LC_R - C_2^2}\left[\frac{1}{2}C_Rn_L^2 + \frac{1}{2}C_Ln_R^2 + C_2n_Ln_R\right].$$

To calculate the free energy, we first calculate the work performed by the external sources to achieve a configuration with $n_L = m_1 - m_2$ and $n_R = m_2 - m_3$ electrons in the system. We consider Eq. (A1) in terms of the voltages on the junctions, V_j, j = 1, 2, 3. For simplicity, we consider, first, the case without V_G, *i.e.*, $C_{G1/2} = 0$:

$$\begin{aligned} V_1 &= \frac{1}{\Sigma}\left[C_2C_3V(t) + em_1(C_2 + C_3) - em_2C_3 - em_3C_2\right] \\ V_2 &= \frac{1}{\Sigma}\left[C_1C_3V(t) - em_1C_3 - em_2(C_3 + C_1) - em_3C_1\right] \\ V_3 &= \frac{1}{\Sigma}\left[C_1C_2V(t) - em_1C_2 - em_2C_1 + em_3(C_1 + C_2)\right], \end{aligned} \quad \text{(A2)}$$

where we have defined $\Sigma = C_LC_R - C_2^2$. We now calculate the work done by the external source, $V(t) = V_S$. For instance, the work done by V_S for one electron to tunnel through the first junction, $m_1 \to m_1 + 1$, is given by $\delta W_1 = V_S\delta q_1$, where $\delta q_1 = -|e| + C_1\delta V_1$. From Eq. (A2), we see that

$$\delta V_1 = |e|\frac{C_2 + C_3}{\Sigma} \to \delta W_1 = -|e|V_S\frac{C_2C_3}{\Sigma}.$$

In general, the work performed by the external source V_S for a tunneling event through the i-th junction is

$$\delta W_i = -|e|V_S\frac{(\varepsilon_{ijk})^2C_jC_k}{2\Sigma},$$

where ε_{ijk} is the Levi-Civita antisymmetric tensor. For the finite $C_{G1/2}$ case, we have (now $C_L = C_1 + C_2 + C_{G1}$ and $C_R = C_2 + C_3 + C_{G2}$):

$$\begin{aligned} V_1 &= \frac{1}{\sigma}\left[C_R(C_L - C_1)V(t) - (C_RC_{G1} + C_2C_{G2})V_G + \right. \\ &+ \left. |e|(m_1C_R - m_2(C_R - C_2) - m_3C_2)\right]. \end{aligned}$$

We can now write an expression for δW_i in terms of the capacitances,

$$\begin{aligned} \delta W_1 &= -|e|V_S\frac{C_2C_3 + C_{G1}C_R + C_{G2}C_2}{\Sigma}; \\ \delta W_2 &= -|e|V_S\frac{C_1C_3 + C_1C_{G2}}{\Sigma}; \\ \delta W_3 &= -|e|V_S\frac{C_1C_2}{\Sigma}. \end{aligned}$$

Likewise, the work performed by the gate in the tunneling process through the i-th junction, $\delta W_{Gi} = V_G[\delta q_{G1}(m_i \to m_i + 1) + \delta q_{G2}(m_i \to m_i + 1)]$:

$$\begin{aligned} \delta W_{G1} &= |e|V_G\frac{C_{G1}C_R + C_{G2}C_2}{\Sigma}; \\ \delta W_{G2} &= |e|V_G\frac{C_{G2}(C_L - C_2) - C_{G1}(C_R - C_2)}{\Sigma}; \\ \delta W_{G3} &= -|e|V_G\frac{C_{G2}C_L + C_2C_{G1}}{\Sigma}. \end{aligned} \quad \text{(A3)}$$

The electrostatic free energy is then given by $F = U - W$, with $W(\{m_i\}) = \sum m_i(\delta W_i + \delta W_{Gi})$, and, bearing in mind Eq. (3),

$$F(\{n_\alpha, m_i\}) = \frac{e^2}{C_L C_R - C_2^2}\left\{C_R\frac{n_L^2}{2} + C_L\frac{n_R^2}{2} + C_2 n_L n_R - \frac{m_1}{|e|}\left[V_G(C_{G1}C_R + C_{G2}C_2) - V_S[C_2C_3 + C_{G1}C_R + C_{G2}C_2]\right]\right.$$
$$\left. - \frac{m_2}{|e|}\left[V_G(C_{G1}(C_R - C_2) - C_{G2}(C_L - C_2)) + V_S C_1 C_3 + C_1 C_{G2}\right] + \frac{m_3}{|e|}\left[V_G(C_L C_{G2} + C_2 C_{G1}) + V_S C_1 C_2\right]\right\}. \quad \text{(A4)}$$

Appendix B: Transient equations

1. rf excitation

We want to arrive from Eq. (23) to Eq. (24). We use $x_0 = A(\eta)\cos z + B(\eta)\sin z$ and Eq. (19):

$$\frac{\partial x_0}{\partial z} = -A\sin z + B\cos z; \quad \frac{\partial^2 x_0}{\partial z^2} = -A\cos z - B\sin z;$$
$$\frac{\partial^2 x_0}{\partial z \partial \eta} = -\frac{\partial A}{\partial \eta}\sin z + \frac{\partial B}{\partial \eta}\cos z.$$

Also, we need the terms in x_0, x_0^2, and x_0^3 all multiplied by $(1-\cos 2z)$. For the linear terms, we have to evaluate $(1-\cos 2z)x_0$, for the quadratic terms, $(1-\cos 2z)x_0^2$, and, finally, for the cubic ones, $(1-\cos 2z)x_0^3$,

$$(1-\cos 2z)(A\sin z + B\cos z) = \frac{A}{2}(\cos z - \cos 3z) + \frac{B}{2}(3\sin z - \sin 3z)$$
$$(1-\cos 2z)(A\sin z + B\cos z)^2 = \frac{A}{4}(1-\cos 4z) + \frac{AB}{2}(2\sin 2z - \sin 4z) + \frac{B^2}{4}(3 - 2\cos 2z + \cos 4z)$$
$$(1-\cos 2z)(A\sin z + B\cos z)^3 = \frac{A^3}{4}\left(\cos z - \frac{1}{2}\cos 3z - \frac{1}{2}\cos 5z\right) + \frac{3A^2B}{4}\left(\sin z + \frac{1}{2}\sin 3z - \frac{1}{2}\sin 5z\right)$$
$$+ \frac{3AB^2}{4}\left(\cos z - \frac{3}{2}\cos 3z + \frac{1}{2}\cos 5z\right) + \frac{B^3}{4}\left(5\sin z - \frac{5}{2}\sin 3z + \frac{1}{2}\sin 5z\right).$$

Now all we need to do is to substitute the above equations into Eq. (23) and arrange terms, *i.e.*, we obtain an equation of the form:

$$\frac{\partial^2 x_1}{\partial z^2} + x_1 = (\ldots)\sin z + (\ldots)\cos z + \text{nonresonant terms}.$$

For non-resonant terms, we require the coefficients of $\sin z$ and $\cos z$ to vanish. We then get Eq. (24).

2. Superimposed DC excitation

We consider Eq. (25) and as before, expand the solutions in terms of ε, using Eqs. (19), (20), and (22) and arrive at a similar set of equations, only now we have extra terms (in β, β^2),

$$\frac{d^2 x_1}{dz^2} + x_1 + 2\delta_\omega\frac{d^2 x_0}{dz^2} + 2\frac{d^2 x_0}{dz d\eta} + \frac{1}{Q}\frac{dx_0}{dz} +$$
$$+ \ 2\alpha(\sin^2 z + 2\beta\sin z + \beta^2)\left(x_0 - \frac{2\lambda}{d}x_0^2 - \frac{3}{16}x_0^3\right) = 0 \quad \text{(B1)}$$

The last term is a tedious one, giving nine terms, six of which are new. We use

$$\begin{aligned}
2\alpha\sin^2 z x_0 &\simeq \frac{\alpha}{2}[A\cos z + 3B\sin z] \\
-\frac{4\lambda\alpha}{d}\sin^2 z x_0^2 &\simeq -\frac{\lambda\alpha}{2d}[A^2+3B^2] \\
-\frac{6\alpha}{16}\sin^2 z x_0^3 &\simeq -\frac{3\alpha}{64}[A(A^2+3B^2)\cos z + \\
&\quad +B(3A^2+5B^2)\sin z] \\
4\alpha\beta\sin z x_0 &\simeq 2\alpha\beta B \\
-\frac{8\lambda\alpha\beta}{d}\sin z x_0^2 &\simeq -\frac{2\lambda\alpha\beta}{d}B[(A^2+3B^2)\sin z + 2AB\cos z] \\
-\frac{12\alpha}{16}\sin z x_0^3 &\simeq -\frac{9\alpha\beta}{32}B(A^2+B^2) \\
2\alpha\beta^2 x_0 &\simeq 2\alpha\beta^2(A\cos z + B\sin z) \\
-\frac{4\lambda\alpha\beta^2}{d}x_0^2 &\simeq -\frac{2\lambda\alpha\beta^2}{d}(A^2+B^2) \\
-\frac{3\alpha\beta^2}{16}x_0^3 &\simeq -\frac{9\alpha\beta^2}{32}(A^2+B^2)(A\cos z + B\sin z).
\end{aligned}$$

Substituting into Eq. (B1) and again arranging terms in $\sin z$ and $\cos z$,

$$\begin{aligned}
2\frac{\partial A}{\partial\eta} &= -\gamma A - \left(2\delta_\omega - \frac{3\alpha}{2} - 2\alpha\beta^2\right)B - \frac{2\lambda\alpha\beta}{d}(A^2+3B^2) - \\
&\quad -\frac{3\alpha}{64}B[3A^2(1+2\beta^2) + B^2(5+6\beta^2)] \\
2\frac{\partial B}{\partial\eta} &= -\gamma B + \left(2\delta_\omega - \frac{\alpha}{2} - 2\alpha\beta^2\right)A + \frac{4\lambda\alpha\beta}{d}AB + \\
&\quad +\frac{3\alpha}{64}A[A^2(1+6\beta^2) + 3B^2(1+2\beta^2)]
\end{aligned} \tag{B2}$$

Next, we need to evaluate the last nine terms of the equation above, which involves trigonometric operations. The relevant contributions for the dynamics of the system are the terms proportional to $\sin z/p$ and $\cos z/p$ (resonant terms). These are:

$$\alpha x_0\sin^2 z = \frac{\alpha}{4}\left[A(2+\delta_{p,1})\cos\frac{z}{p} + B(2-\delta_{p,1})\sin\frac{z}{p}\right]$$

$$2\beta\alpha x_0\sin z = \beta\alpha\left[A\sin\frac{z}{p} + B\cos\frac{z}{p}\right]\delta_{p,2}$$

3. Subharmonics in the general case

We consider the general case in which the driving frequency is given by $\omega \simeq p + \varepsilon\delta_\omega$ and $x \simeq x_0 + \varepsilon x_1$, giving:

$$\begin{aligned}
\dot{x}(t) &= p\frac{\mathrm{d}x_0}{\mathrm{d}z} + \varepsilon\delta_\omega\frac{\mathrm{d}x_0}{\mathrm{d}z} + \varepsilon\frac{\mathrm{d}x_0}{\mathrm{d}\eta} + \varepsilon p\frac{\mathrm{d}x_0}{\mathrm{d}z} + O(\varepsilon^2), \\
\ddot{x}(t) &= p^2\frac{\mathrm{d}^2x_0}{\mathrm{d}z^2} + 2\varepsilon\delta_\omega p\frac{\mathrm{d}^2x_0}{\mathrm{d}z^2} + 2\varepsilon p\frac{\mathrm{d}^2x_0}{\mathrm{d}\eta\mathrm{d}z} + \varepsilon p^2\frac{\mathrm{d}^2x_1}{\mathrm{d}z^2} + O(\varepsilon^2).
\end{aligned} \tag{B3}$$

So now Eq. (25) is, to lowest order in ε,

$$p^2\frac{\mathrm{d}^2x_0}{\mathrm{d}z^2} + x_0 = 0 \quad\rightarrow\quad x_0 = A(\eta)\cos\frac{z}{p} + B(\eta)\sin\frac{z}{p}.$$

Substituting the expression for x_0 into Eq. (25) to first order in ε, we get

$$\begin{aligned}
&- \frac{2\delta_\omega}{p}\left[A(\eta)\cos\frac{z}{p} + B(\eta)\sin\frac{z}{p}\right] - 2\left[\frac{\mathrm{d}A(\eta)}{\mathrm{d}\eta}\sin\frac{z}{p} - \frac{\mathrm{d}B(\eta)}{\mathrm{d}\eta}\cos\frac{z}{p}\right] - \frac{1}{Q}\left[A(\eta)\sin\frac{z}{p} + B(\eta)\cos\frac{z}{p}\right] \\
&+ 2\alpha(\sin^2 z + 2\beta\sin z + \beta^2)\left(\left[A(\eta)\cos\frac{z}{p} + B(\eta)\sin\frac{z}{p}\right] - \frac{2\lambda}{d}\left[A(\eta)\cos\frac{z}{p} + B(\eta)\sin\frac{z}{p}\right]^2\right. \\
&\left. - \frac{3}{16}\left[A(\eta)\cos\frac{z}{p} + B(\eta)\sin\frac{z}{p}\right]^3\right) = 0
\end{aligned} \tag{B4}$$

$$\beta\alpha^2 x_0 = \beta\alpha^2\left[A\sin\frac{z}{p} + B\cos\frac{z}{p}\right]$$

$$\frac{\lambda\alpha x_0^2}{2d}\sin^2 z = \frac{\lambda\alpha}{16d}\left[(B^2-A^2)\cos\frac{z}{p} + AB\sin\frac{z}{p}\right]\delta_{p,3/2}$$

$$\frac{\lambda\alpha\beta}{d}x_0^2\sin z = \frac{\lambda\alpha\beta}{4d}\left[2AB\cos\frac{z}{p} + (A^2-B^2)\sin\frac{z}{p}\right]\delta_{p,3}$$

$$\frac{\lambda\alpha\beta^2}{2d}x_0^2\sin z \rightarrow \text{no contributions}$$

$$-\frac{3\alpha\beta^2x_0^3}{16} = -\frac{9\alpha\beta^2}{64}(A^2+B^2)\left[A\sin\frac{z}{p}+B\cos\frac{z}{p}\right]$$

$$\begin{aligned}-\frac{3\alpha x_0^3}{16}\sin^2 z &= -\frac{3\alpha}{128}\left[A\cos\frac{z}{p}\left(3(A^2+B^2)(1-\frac{3}{2}\delta_{p,1})-\frac{1}{2}(3A^2-B^2)\delta_{p,2}\right)\right.\\ &\left.+B\sin\frac{z}{p}\left(3(A^2+B^2)(1-\frac{3}{2}\delta_{p,1})-\frac{1}{2}(3A^2-B^2)\delta_{p,2}\right)\right]\end{aligned}$$

$$\begin{aligned}-\frac{3\alpha x_0^3}{16}\sin^2 z &= -\frac{3\alpha}{128}\left[A\sin\frac{z}{p}\left(3(A^2+B^2)\delta_{p,2}+(A^2-3B^2)\delta_{p,4}\right)\right.\\ &\left.+B\cos\frac{z}{p}\left(3(A^2+B^2)\delta_{p,2}+(3A^2-B^2)\delta_{p,4}\right)\right]\end{aligned}$$

As we did before, we can now arrange all the terms in Eq. (B4) as coefficients of $\sin z/p$ and $\cos z/p$, resulting in our desired equation,

$$\begin{aligned}2\frac{\partial A}{\partial\eta} &= -A(\gamma-\beta\alpha\delta_{p,2})-B\left(\frac{2\delta_\omega}{p}-\frac{\alpha}{4}(2+\delta_{p,1}+4\beta^2)\right)+AB\frac{\lambda\alpha}{8d}\delta_{p,3/2}+(A^2-B^2)\frac{\beta\lambda\alpha}{4d}\delta_{p,3}\\ &-\frac{3\alpha}{256}\left[B(A^2+B^2)(6+12\beta^2+3\delta_{p,1})+B(3A^2-B^2)\delta_{p,2}+6A(A^2+B^2)\delta_{p,2}+2A(A^2-3B^2)\delta_{p,4}\right]\\ 2\frac{\partial B}{\partial\eta} &= -B(\gamma+\beta\alpha\delta_{p,2})+A\left(\frac{2\delta_\omega}{p}-\frac{\alpha}{4}(2-\delta_{p,1}+4\beta^2)\right)+(A^2-B^2)\frac{\lambda\alpha}{16d}\delta_{p,3/2}-AB\frac{\lambda\beta\alpha}{2d}\delta_{p,3}\\ &+\frac{3\alpha}{256}\left[A(A^2+B^2)(6+12\beta^2-3\delta_{p,1})-A(A^2-3B^2)\delta_{p,2}+6B(A^2+B^2)\delta_{p,2}+2B(3A^2-B^2)\delta_{p,4}\right]\end{aligned} \tag{B5}$$

4. Transients in the Coulomb blockade limit

We substitute again the general solution, $x(t)\simeq x_0+\varepsilon x_1$, in Eq. (29), along with the expression for $\langle n(t)\rangle$ given in (30). The equation of motion now reads

$$\begin{aligned}&\frac{\partial^2 x_1}{\partial z^2}+x_1+2\frac{\partial^2 x_0}{\partial z\partial\eta}+2\delta_\omega\frac{\partial^2 x_0}{\partial z^2}-\frac{1}{Q_1}\frac{\partial x_0}{\partial z}+\\ &\alpha_1'(\sin\omega t+\beta)(n_{\rm av}+4n_0(\cos\omega_0 t-\cos 3\omega_0 t)/\pi) = 0\end{aligned} \tag{B6}$$

As before, we evaluate the equation of motion with $x_0(t)\simeq A(\eta)\cos z/p+B(\eta)\sin z/p$, using (B1). Inserting this into Eq. (B6) and considering the resonant terms, with $\omega t=z$ and $\omega_0 t=z/p$, we obtain

$$-2\frac{\delta_\omega}{p}A\cos\frac{z}{p}-2\frac{\delta_\omega}{p}B\sin\frac{z}{p}-2\frac{dA}{d\eta}\sin\frac{z}{p}+2\frac{dB}{d\eta}\cos\frac{z}{p}-\gamma_1 A\sin\frac{z}{p}+\gamma_1 B\cos\frac{z}{p}+\alpha_1'\beta n_{\rm av}$$
$$+\alpha_1'\beta n_0\cos\frac{z}{p}+\alpha_1' n_{\rm av}\sin\frac{z}{p}\delta_{p,1}-\frac{1}{2}\alpha_1' n_0\sin\frac{z}{p}\delta_{p,2}-\frac{1}{6}\alpha_1' n_0\sin\frac{z}{p}(\delta_{p,4}-\delta_{p,2}) \;=\; \ddot{x}_1+x_1. \qquad \text{(B7)}$$

Arranging the terms in $\sin z/p$ and $\cos z/p$, we get Eq. (31).

In the small oscillations limit, $n(t)$ "follows" linearly the mechanical oscillations of the islands, $n(t)\simeq n_0\sin\omega_0 t$, giving a different set of equations,

$$\begin{aligned} 2\frac{dA}{d\eta} &= -\gamma_1 A-\frac{2\delta_\omega}{p}B+\alpha_1'\beta n_0,\\ 2\frac{dB}{d\eta} &= -\gamma_1 B+\frac{2\delta_\omega}{p}A-n_0\frac{\alpha_1'}{3}\delta_{p,2}. \end{aligned} \qquad \text{(B8)}$$

[1] D. V. Scheible and R. H. Blick, *Applied Physics Letters*, **84**, 4632–4634, (2004).

[2] C. Kim, J. Park, and R. H. Blick, *Phys. Rev. Lett.*, **105**, 067204–067207, (2010).

[3] C. Kim, M. Prada, and R. H. Blick, *ACS Nano*, **6**, 651–655, (2012).

[4] G. Cohen, V. Fleurov and K. Kikoin, *Phys. Rev. B*, **79**, 245307, (2009).

[5] C. Kim, M. Prada, G. Platero and R. H. Blick, (*unpublished*).

[6] S P Beeby, M J Tudor and N M White, *Meas. Sci. Technol* **17**, 175 (2006).

[7] J. Li, H. Yu, S. M. Wong, G. Zhang, X. Sun, P. G.–Q. Lo, and D.–L. Kwong *Appl. Phys. Lett.* **95**, 033102–033104 (2009).

[8] Arunkumar Subramanian, Andreas R. Alt, Lixin Dong, Bradley E. Kratochvil, Colombo R. Bolognesi, and Bradley J. Nelson. *ACS Nano*, **3**, 2953–2964 (2009).

[9] R. H Blick, H. Qin, H.–S. Kim, and R. Marsland, *New Journal of Physics*, **9** 241 (2007).

[10] I. Mahboob, E. Flurin, K. Nishiguchi, A. Fujiwara, and H. Yamaguchi, *Nat. Commun.*, **2**, 198 (2011).

[11] M. D. LaHaye, J. Suh, P. M. Echternach, K. C. Schwab, and M. L. Roukes, *Nature*, **459**, 960–964 (2009).

[12] Rongrui He, X. L. Feng, M. L. Roukes, and Peidong Yang. *Nano Letters*, **8**, 1756–1761 (2008).

[13] Sebastian T. Bartsch, Andrea Lovera, Daniel Grogg, and Adrian M. Ionescu. *ACS Nano* **6**, 256–264 (2012).

[14] László Oroszlány, Viktor Zólyomi, and Colin J. Lambert *ACS Nano* **4**, 7363-7366 (2010).

[15] M. Law, L. E. Greene, J. C. Johnson, R. Saykally, and P. Yang, *Nat. Mater.* **4**, 455 (2005); M. D. Kelzenberg, D. B. Turner-Evans, B. M. Kayes, M. A. Filler, M. C. Putnam, N. S. Lewis, and H. A. Atwater, *Nano Lett.* **8**, 710 (2008).

[16] D. Rugar, R. Budakian, H. J. Mamin, and B. W. Chui, *Nature*, **430** 329–332, (2004).

[17] D. Rugar and P. Grütter, *Phys. Rev. Lett.*, **67** 699–702, (1991).

[18] A. K. Naik, M. S. Hanay, W. K. Hiebert, X. L. Feng, M. L. and Roukes, *Nat. Nano*, **4**, 445–450 (2009).

[19] F. Pistolesi and R. Fazio, *Phys. Rev. Lett.*, **94**, 036806–036809 (2005).

[20] F. Haupt, F. Cavaliere, R. Fazio, and M. Sassetti, *Phys. Rev. B*, **74**, 205328 (2006).

[21] M. Merlo, F. Haupt, F. Cavaliere, and M. Sassetti *New J. Phys.*, **10**, 023008 (2008).

[22] K.–H. Ahn, H. C. Park, J. Wiersig, and H. Jongbae, *Phys. Rev. Lett.*, 97, 216804–216807 (2006).

[23] L. Guillermo Villanueva, Rassul B. Karabalin, Matthew H. Matheny, Eyal Kenig, Michael C. Cross, and Michael L. Roukes. *Nano Letters*, **11**, 5054–5059 (2011).

[24] Daniel Midtvedt, Yury Tarakanov, and Jari Kinaret. *Nano Letters*, **11**, 1439–1442 (2011).

[25] A N Cleland, *Foundations of Nanomechanics* (Springer Verlag, Berlin, 2003).

[26] M. A. Hopcroft, W. D. Nix, and T. W. Kenny, *J. Microelectromech. Syst.* **19**, 229 (2010).

[27] I. O. Kulik and R. .I Shekhter. *Sov. Phys. JETP*, **41** 308, (1975).

[28] D. V. Averin, and K. K. Likharev, *J. Low Temp. Phys.* **62**, 345 (1986).

[29] C. Weiss and W. Zwerger, *Europhysics Letters*, **47**, 97, (1999).

[30] W. G. van der Wiel, S. De Franceschi, J. M. Elzerman, T. Fujisawa, S. Tarucha, and L. P. Kouwenhoven. *Rev. Mod. Phys.*, **75**, 1, (2002).

[31] A H Nayfeh and D T Mook, *Nonlinear Oscillations*. (Wiley Interscience, New York, 1970).

[32] M. Prada, and G. Platero, (*unpublished*).

[33] D. V. Scheible, C. Weiss, J. P. Kotthaus, and R. H. Blick, *Phys. Rev. Lett.*, **93**, 186801, (2004).